

Constraints on millicharged neutrinos via analysis of data from atomic ionizations with germanium detectors at sub-keV sensitivities

Jiunn-Wei Chen,^{1,2} Hsin-Chang Chi,³ Hau-Bin Li,⁴ C.-P. Liu,³ Lakhwinder Singh,^{4,5,*} Henry T. Wong,^{4,†} Chih-Liang Wu,^{1,4,‡} and Chih-Pan Wu¹

¹*Department of Physics, National Taiwan University, Taipei 10617, Taiwan*

²*National Center for Theoretical Sciences and Leung Center for Cosmology and Particle Astrophysics, National Taiwan University, Taipei 10617, Taiwan*

³*Department of Physics, National Dong Hwa University, Shoufeng, Hualien 97401, Taiwan*

⁴*Institute of Physics, Academia Sinica, Taipei 11529, Taiwan*

⁵*Department of Physics, Banaras Hindu University, Varanasi 221005, India*

(Received 23 May 2014; published 24 July 2014)

With the advent of detectors with sub-keV sensitivities, atomic ionization has been identified as a promising avenue to probe possible neutrino electromagnetic properties. The interaction cross sections induced by millicharged neutrinos are evaluated with the *ab initio* multiconfiguration relativistic random-phase approximation. There is significant enhancement at atomic binding energies compared to that when the electrons are taken as free particles. Positive signals would distinctly manifest as peaks at specific energies with known intensity ratios. Selected reactor neutrino data with germanium detectors at an analysis threshold as low as 300 eV are studied. No such signatures are observed, and a combined limit on the neutrino charge fraction of $|\delta_Q| < 1.0 \times 10^{-12}$ at 90% confidence level is derived.

DOI: 10.1103/PhysRevD.90.011301

PACS numbers: 14.60.Lm, 13.15.+g, 13.40.Gp

The physical origin and experimental consequences of finite neutrino masses and mixings [1] are not fully understood. Investigations on anomalous neutrino properties and interactions [1] are crucial to address these fundamental questions and may provide hints or constraints to new physics beyond the Standard Model (SM). An avenue is on the studies of possible neutrino electromagnetic interactions [1–3], which, in addition, offer the potentials to differentiate between Majorana and Dirac neutrinos. The neutrino electromagnetic form factors in C , P , and T -conserving theories can be formulated as

$$\Gamma_{\text{em}}^\mu \equiv F_1 \cdot \gamma^\mu + F_2 \cdot \sigma^{\mu\nu} \cdot q_\nu, \quad (1)$$

with

$$F_1 = \delta_Q \cdot e_0 + \frac{1}{6} \cdot q^2 \cdot \langle r_\nu^2 \rangle, \quad (2)$$

and

$$F_2 = (-i) \cdot \frac{\mu_\nu}{2 \cdot m_e}, \quad (3)$$

where γ^μ and $\sigma^{\mu\nu}$ are the standard QED matrices; e_0 and m_e are the electron charge and mass, respectively; $q = (q_0, \vec{q})$ is the 4-momentum transfer; while the neutrino properties are parametrized by the neutrino fractional charge relative to the electron (δ_Q —commonly referred to as “neutrino

millicharge” in the literature), the neutrino charge radius ($\langle r_\nu^2 \rangle$), and the anomalous neutrino magnetic moment (μ_ν) [2,3] in units of the Bohr magneton μ_B . The F_1 and F_2 terms characterize neutrino interactions without and with a change of the helicity states, respectively. The studies of δ_Q and $\langle r_\nu^2 \rangle$ should in general be coupled to those due to SM-electroweak interactions to account for the possible interference effects among them. For completeness, we note that two additional form factors are possible [3]: the electric dipole moments in theories violating both P and T symmetries and the anapole moments in P -violating theories.

The theme of this article is to report a new direct laboratory limit on $|\delta_Q|$. The searches are based on $\bar{\nu}_e$ emitted from the nuclear power reactor via atomic ionization [4], an interaction channel considered for the first time in this process. The cross section is derived using the Multi-Configuration Relativistic Random-Phase Approximation (MCRRPA) theory [5,6]. As will be demonstrated in Fig. 1(b), the bounds on event rates from δ_Q -induced atomic interactions $[\bar{\nu}_e\text{-A}(\delta_Q)]$,

$$\bar{\nu}_e + \text{A} \rightarrow \bar{\nu}_e + \text{A}^+ + e^-, \quad (4)$$

to be probed in this work (~ 1 count $\text{kg}^{-1} \text{keV}^{-1} \text{day}^{-1}$ at an energy transfer of $T \sim 0.1\text{--}10$ keV) far exceed those due to SM interactions as well as $\langle r_\nu^2 \rangle$ -induced processes at its current limits [7], such that these effects and their interference can be neglected in our analysis.

The origin of electric charge quantization and whether it is exact is one of nature’s profound mysteries. Many theories [9], such as extra dimensions, magnetic

*lakhwinder@phys.sinica.edu.tw

†htwong@phys.sinica.edu.tw

‡b97b02002@ntu.edu.tw

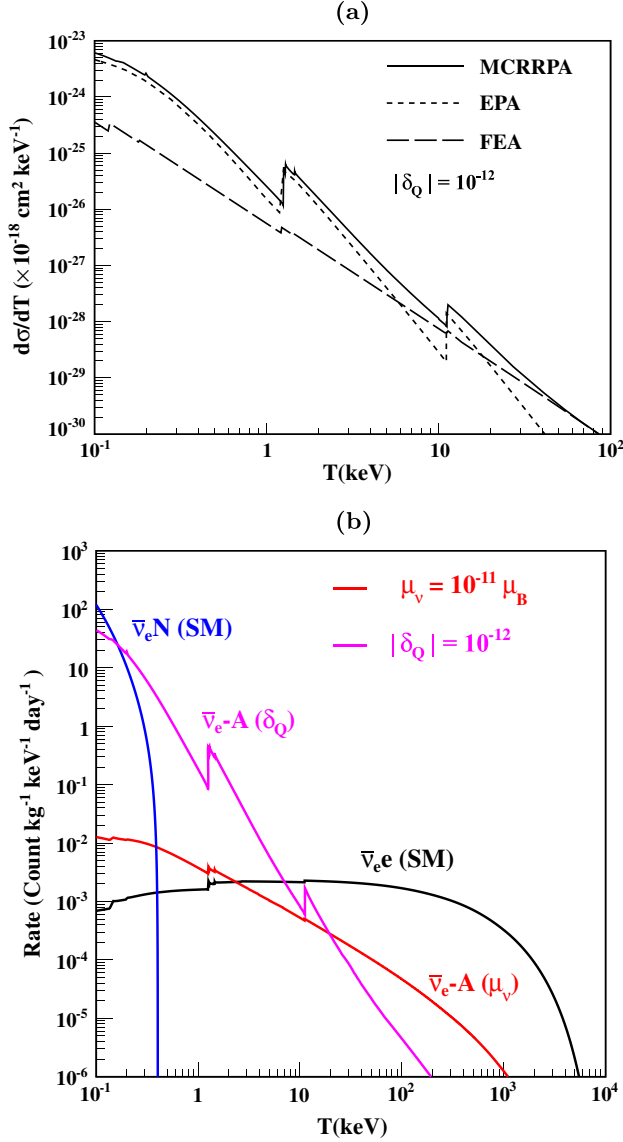


FIG. 1 (color online). The differential cross sections $\bar{\nu}_e$ -A(δ_Q) on Ge due to $|\delta_Q| = 10^{-12}$ —(a) with monochromatic $E_\nu = 1$ MeV, derived with the FEA, EPA, and MCRRPA methods and (b) with typical reactor spectrum at a flux of $\phi(\bar{\nu}_e) = 10^{13} \text{ cm}^{-2} \text{ s}^{-1}$, where contributions from SM $\bar{\nu}_e$ -e and $\bar{\nu}_e$ -nucleus (N) as well as those of $\mu_\nu = 10^{-11} \mu_B$ are overlaid. Standard quenching factors [8] are used to account for observable ionizations in nuclear recoils. The contribution to $\bar{\nu}_e$ -e from $\langle r_\nu^2 \rangle$ at its current upper bound is only a fraction of that from SM and is not shown.

monopoles, and grand unified theories, provide elegant solutions, but they remain speculative. Electric charges are quantized in the SM due to $U(1)$ gauge invariance and anomaly cancellation [10,11], implying $\delta_Q = 0$. However, charge quantization is no longer ensured in many extensions of the SM [11,12]. For example, in theories with right-handed neutrinos and Dirac mass terms, electric charge is no longer quantized, and δ_Q can assume an arbitrary value due to a hidden $U(1)$ symmetry for which

the conserved charge is the difference of baryon and lepton numbers or $B - L$. Charge quantization can be restored by introducing additional conditions such as Majorana mass terms that break the $U(1)$ symmetry [11]. Neutrinos with finite charge will necessarily imply they are Dirac particles.

Model-dependent astrophysics bounds [1,13] ranging at $|\delta_Q| < 10^{-13}$ – 10^{-15} are derived from stellar luminosity and cooling, as well as the absence of anomalous timing dispersion of the neutrino events in SN 1987A. The most stringent indirect limit is $|\delta_Q| < 3 \times 10^{-21}$ [13], inferred from constraints on the neutrality of the hydrogen atoms and the neutrons [14] and assuming charge conservation in neutron beta decay. Earlier efforts with direct laboratory experiments placed constraints $|\delta_Q| < \text{few} \times 10^{-12}$ [15,16] through the extrapolations of the μ_ν results from reactor $\bar{\nu}_e$ experiments [17,18] using simplistic scaling relationships and neglecting atomic effects.

The conventional way of evaluating the effects due to Γ_{em}^μ is with the free electron approximation (FEA). The corresponding differential cross section for δ_Q -induced neutrino–electron scattering [15,16] due to an incoming neutrino of energy E_ν at $T \ll E_\nu$ is

$$\left(\frac{d\sigma}{dT}\right)_{\text{FEA}} = \delta_Q^2 \left[\frac{2\pi\alpha_{\text{em}}^2}{m_e} \right] \left[\frac{1}{T^2} \right], \quad (5)$$

where α_{em} is the fine structure constant. The $(1/T^2)$ dependence is different from that of $(1/T)$ for μ_ν . With the advent of low-energy detectors sensitive to the energy range of atomic transitions and binding energies ($T < 10$ keV), FEA is no longer adequate, and atomic ionization effects have to be taken into account [4]. Cross sections of μ_ν -induced ν -atom scattering have been formulated [6,19,20] by various authors.

The cross section $\bar{\nu}_e$ -A(δ_Q) is analogous to that induced by relativistic charged leptons and can be described at atomic energies by the equivalent photon approximation (EPA) [21],

$$\left(\frac{d\sigma}{dT}\right)_{\text{EPA}} = \delta_Q^2 \left[\frac{2\alpha_{\text{em}}}{\pi} \right] \left[\frac{\sigma_\gamma(T)}{T} \right] \log \left[\frac{E_\nu}{m_\nu} \right], \quad (6)$$

where m_ν is the neutrino and $\sigma_\gamma(T)$ is the photoelectric cross section by a real photon of energy T [22]. The divergence at $m_\nu \rightarrow 0$ is expected in Coulomb scattering, and some cutoff schemes are necessary. The Debye length for solid-Ge ($0.68 \mu\text{m}$ or 0.29 eV), which characterizes the scale of screen Coulomb interaction, is chosen. This may introduce an uncertainty of $\sim 20\%$ to the normalization if m_ν would be replaced by other values related to neutrino mass bounds. The EPA method neglects the contributions from the longitudinal polarization of the virtual photons and hence would deviate from the correct results as T increases. It fails to describe ionizations by μ_ν , $\langle r_\nu^2 \rangle$, or electroweak interactions [20].

We adopted the MCRRPA theory [5] as an *ab initio* approach [6] to provide an improved description of the atomic many-body effects. This becomes relevant for data from Ge detectors at sub-keV sensitivities. The MCRRPA theory is a generalization of relativistic random-phase approximation (RRPA) by the use of a multiconfiguration wave function as the reference state. It has been successfully applied to photoexcitation, photoionization, and μ_ν -induced ionization of divalent or quasivalent atomic systems [5,6]. There are various aspects where MCRRPA improves over the time-dependent Hartree–Fock (HF) approximation in describing the structures and transitions of Ge:

- (i) The Ge atom has two valence $4p$ electrons. Its ground state, a 3P_0 state, can be formed by either a $4p_{\frac{1}{2}}^2$ or a $4p_{\frac{3}{2}}^2$ valence configuration. This entails the necessity of a multiconfiguration reference state.
- (ii) With an atomic number of $Z = 32$, the relativistic corrections, in power of $Z\alpha_{\text{em}} \sim 1/4$, can no longer be ignored. By solving a relativistic wave equation, the leading relativistic effects are included non-perturbatively from the onset.
- (iii) The two-body correlation beyond HF is generally important in building excited states. The RRPA is an established method in accounting for two-body correlation, having nice features such as treating the reference and excited states on the same footing and preserving gauge invariance. In combination with the multiconfiguration reference state, configuration mixing due to two-body correlation is also taken into account.

The MCRRPA results of this work are benchmarked by the measured photoabsorption cross section of solid Ge from real photons [6,22]. As demonstrated in Fig. 2, the calculations successfully reproduce the data to an accuracy of within 5% at energy transfer larger than 100 eV, where the inner-shell electrons of Ge ($3p$ and below) provide the dominant contributions. The deviations originate from the small contributions of the outer-shell electrons. At lower energy, the solid state effects start to play a role, since Ge is fabricated as semiconductor crystals in ionization detectors.

The derived differential cross section for $\bar{\nu}_e$ -A(δ_Q) on Ge under various schemes is depicted in Fig. 1(a) with a monochromatic incident neutrino at $E_\nu = 1$ MeV, a typical range for reactor $\bar{\nu}_e$. The FEA scheme is expected to provide good descriptions at energy transfer larger than the atomic binding energy scale, while EPA at $q^2 \rightarrow 0$. The MCRRPA results converge to these benchmarks: $T > 50$ keV for FEA and $T < 1$ keV for EPA, confirming the method covers a wide range of validity. Two features are particularly noteworthy:

- (i) There is an order-of-magnitude enhancement in the MCRRPA or EPA cross section over FEA at low energy when atomic effects are taken into account. This behavior is opposite to that for μ_ν -induced interactions [6,19] where the cross section is

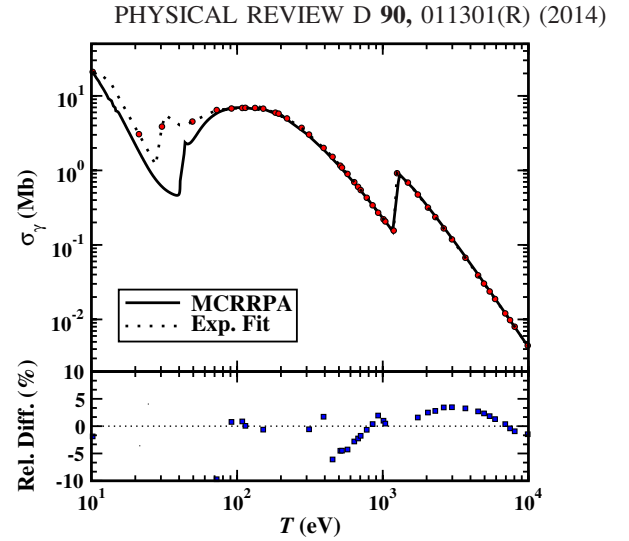


FIG. 2 (color online). Germanium photoionization cross section. The solid curve corresponds to the results of MCRRPA calculation. The dotted line is a fit to experimental data taken from Ref. [22]. The relative differences (excess of MCRRPA results over data relative to the measurements) are shown in the lower panel.

suppressed, the origin of which is discussed in Ref. [20].

- (ii) There exists a unique “smoking gun” signature for $\bar{\nu}_e$ -A(δ_Q), through the observation of K- and L-shell peaks at the specific binding energies and with known intensity ratios. Both features favor the use of detectors with low threshold at sub-keV energy and yet possess good resolution to resolve peaks and other structures at such energy.

To be comparable with experimental data, the differential cross sections are convoluted with the neutrino spectrum $d\phi/dE_\nu$ to provide the observable spectrum of event rates (R) as function of T ,

$$\frac{dR}{dT} = \rho_e \int_{E_\nu} \left[\frac{d\sigma}{dT} \right] \left[\frac{d\phi}{dE_\nu} \right] dE_\nu, \quad (7)$$

where ρ_e is the electron number density per unit target mass. The MCRRPA spectrum for $[\bar{\nu}_e$ -A(δ_Q)] with Ge at a typical reactor neutrino flux of $\phi(\bar{\nu}_e) = 10^{13} \text{ cm}^{-2} \text{ s}^{-1}$ is depicted in Fig. 1(b) and is compared with those of μ_ν -induced and SM $\bar{\nu}_e$ -e and $\bar{\nu}_e$ -nucleus coherent scatterings [23]. It can be seen that low threshold detectors can greatly enhance the sensitivities in most of the channels.

The previous analyses [15,16] with FEA are repeated using full spectral data via standard statistical procedures. Comparisons of the results listed in Table I show discrepancies and indicate inadequacies of the scaling approach. Also displayed are the analyses of reactor $\bar{\nu}_e$ data [8,17,18] using the MCRRPA spectrum of Fig. 1(b). No evidence on $\bar{\nu}_e$ -A(δ_Q) is observed, and limits of $|\delta_Q|$ at 90% C.L. are derived. In particular, we illustrate the results from

TABLE I. Summary of experimental limits on millicharged neutrino at 90% C.L. with selected reactor neutrino data. “This work” compares data with results from FEA and MCRPPA calculations via a complete analysis, while “previous analysis” is based on extrapolations from μ_ν results using simplistic scaling relations to the FEA spectra. The projected sensitivity of measurements at the specified experimental parameters is also shown.

| Data set | Reactor- $\bar{\nu}_e$ flux ($\times 10^{13} \text{ cm}^{-2} \text{ s}^{-1}$) | Data strength reactor ON/OFF (kg-days) | Analysis threshold (keV) | $ \delta_Q $ 90% C.L. limits ($< \times 10^{-12}$) | | |
|-----------------------------|--|--|--------------------------------|--|-----------|-------------|
| | | | | previous analysis FEA | This work | |
| | | | | | FEA | MCRPPA |
| TEXONO 1 kg Ge [17] | 0.64 | 570.7/127.8 | 12 | 3.7 [15] | 14 | 8.8 |
| GEMMA 1.5 kg Ge [18] | 2.7 | 1133.4/280.4 | 2.8 | 1.5 [16] | 2.1 | 1.1 |
| TEXONO Point-Contact Ge [8] | 0.64 | 124.2/70.3 | 0.3 | ... | ... | 2.1 |
| Projected Point-Contact Ge | 2.7 | 800/200 | 0.1 | ... | ... | ~ 0.06 |

point-contact Ge detectors with sub-keV sensitivities at an analysis threshold of 300 eV [8]. The detectors are deployed by the TEXONO experiment at Kuo-Sheng Reactor Neutrino Laboratory [7,17] for the studies of light weakly interacting massive particle (WIMP) dark matter and $\bar{\nu}_e$ -nucleus coherent scatterings. Typical spectra are depicted in Fig. 3. The “raw” spectrum is due to all events prior to background suppression, while the “selected” ones are those of candidate events having anticoincidence with the cosmic-ray and anti-Compton detectors. Various lines from internal x-ray emissions due to cosmic-induced internal radioactivity can be observed. The low-energy portion of the candidate spectrum is displayed in the inset.

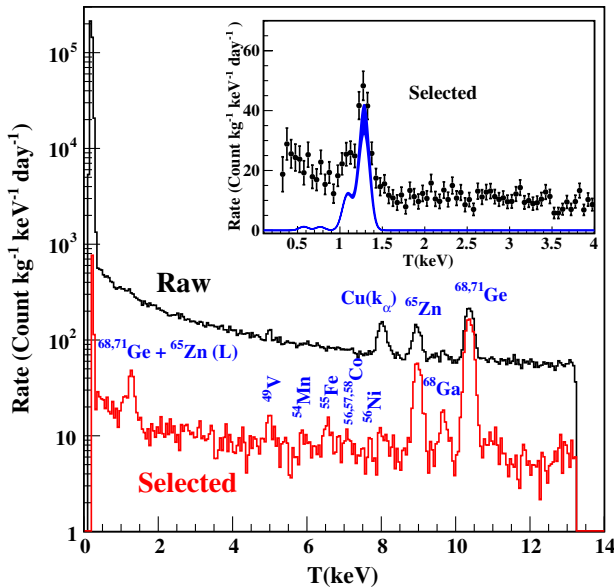


FIG. 3 (color online). Typical spectra from point-contact Ge detectors at the Kuo-Sheng Reactor Neutrino Laboratory. The “selected” spectra are due to events after anticoincidence with the cosmic-ray and anti-Compton detectors. The peaks are due to internal radioactivity. The low-energy spectrum is expanded in the inset. Intensities of the L-shell x rays can be independently derived from the higher-energy K-shell peaks.

The peaks are from the L-shell x rays, where the intensities can be quantitatively accounted for with the higher-energy K-shell peaks. Data taken in different reactor periods are combined and compared with $\bar{\nu}_e$ -A(δ_Q) from MCRPPA. Depicted in Fig. 4 is the reactor ON-OFF residual spectrum with 124.2 (70.3) kg-days of ON (OFF) data. The best-fit solution with the 2σ uncertainty band is superimposed. A limit of $|\delta_Q| < 2.1 \times 10^{-12}$ at 90% C.L. is derived.

The various bounds derived from the MCRPPA analysis shown in Table I can be statistically combined. The overall limit from these reactor neutrino data is

$$|\delta_Q| < 1.0 \times 10^{-12} \quad (8)$$

at 90% C.L. The projected sensitivity for a measurement at an achieved flux and data strength [18] together with 100 eV detector threshold targeted for next generation of experiments [23] would be $|\delta_Q| \sim 6 \times 10^{-14}$.

The MCRPPA theory improves descriptions on neutrino electromagnetic effects at atomic energy scales over previous techniques. Possible charge-induced interactions show enhancement at atomic binding energies and would

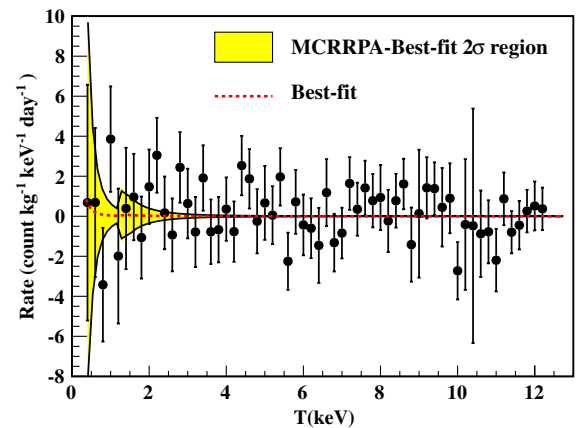


FIG. 4 (color online). Analysis of $\bar{\nu}_e$ millicharge with data from point-contact Ge detectors [8], showing the reactor ON-OFF spectrum with 124.2 (70.3) kg-days of ON (OFF) data. The best-fit function with its 2σ uncertainty band is superimposed.

manifest as peaks with known intensity ratios. Novel Ge-detectors with sub-keV sensitivities and superb energy resolution are ideal to study these effects. We plan to extend our studies to neutrinos at different kinematics regimes, as well as to possible electromagnetic interactions with WIMPs as nonrelativistic particles.

This work is supported by the Academia Sinica Investigator Award 2011-15 (H. T. W.), as well as Contracts No. 102-2112-M-001-018 (L. S. and H. B. L.), No. 102-2112-M-002-013-MY3 (J. W. C., C. L. W., C. P. W.), and No. 102-2112-M-259-005 (C. P. L.) from the Ministry of Science and Technology, Taiwan.

-
- [1] J. Beringer *et al.* (Particle Data Group), *Phys. Rev. D* **86**, 010001 (2012), reviews at p. 177 and p. 622 and references therein.
- [2] B. Kayser, *Phys. Rev. D* **26**, 1662 (1982); J. F. Nieves, *Phys. Rev. D* **26**, 3152 (1982); R. Shrock, *Nucl. Phys.* **B206**, 359 (1982); P. Vogel and J. Engel, *Phys. Rev. D* **39**, 3378 (1989); H. T. Wong and H. B. Li, *Mod. Phys. Lett. A* **20**, 1103 (2005); N. Bell, V. Cirigliano, M. Ramsey-Musolf, P. Vogel, and M. Wise, *Phys. Rev. Lett.* **95**, 151802 (2005).
- [3] C. Broggini, C. Giunti, and A. Studenikin, *Adv. High Energy Phys.* **2012**, 459526 (2012); C. Giunti and A. Studenikin, arXiv:1403.6344.
- [4] S. A. Fayans, V. Yu. Dobretsov, and A. B. Dobrotsvetov, *Phys. Lett. B* **291**, 1 (1992); G. J. Gounaris, E. A. Paschos, and P. I. Porfyriads, *Phys. Lett. B* **525**, 63 (2002); H. T. Wong, H. B. Li, and S. T. Lin, *Phys. Rev. Lett.* **105**, 061801 (E) (2010); arXiv:1001.2074v3.
- [5] K. N. Huang and W. R. Johnson, *Phys. Rev. A* **25**, 634 (1982); K. N. Huang, *Phys. Rev. A* **26**, 734 (1982).
- [6] J.-W. Chen, H.-C. Chi, K.-N. Huang, C.-P. Liu, H.-T. Shiao, L. Singh, H. T. Wong, C.-L. Wu, and C.-P. Wu, *Phys. Lett. B* **731**, 159 (2014), and references therein.
- [7] M. Deniz *et al.*, *Phys. Rev. D* **81**, 072001 (2010).
- [8] H. T. Wong, *Int. J. Mod. Phys. D* **20**, 1463 (2011); H. B. Li *et al.*, *Phys. Rev. Lett.* **110**, 261301 (2013); *Astropart. Phys.* **56**, 1 (2014).
- [9] O. Klein, *Nature (London)* **118**, 516 (1926); P. A. M. Dirac, *Proc. R. Soc. A* **133**, 60 (1931); J. C. Pati and A. Salam, *Phys. Rev. D* **10**, 275 (1974); H. Georgi and S. L. Glashow, *Phys. Rev. Lett.* **32**, 438 (1974).
- [10] G. C. Joshi, H. Lew, and R. R. Volkas, *Mod. Phys. Lett. A* **05**, 2721 (1990); R. Foot, H. Lew, and R. R. Volkas, *J. Phys. G* **19**, 361 (1993).
- [11] K. S. Babu and R. N. Mohapatra, *Phys. Rev. Lett.* **63**, 938 (1989); *Phys. Rev. D* **41**, 271 (1990).
- [12] B. Holdom, *Phys. Lett.* **166B**, 196 (1986); R. Foot, H. Lew, and R. R. Volkas, *Phys. Lett. B* **272**, 67 (1991); I. Antoniadis and K. Benakli, *Phys. Lett. B* **295**, 219 (1992); A. Yu. Ignatiev and G. C. Joshi, *Phys. Lett. B* **381**, 216 (1996).
- [13] G. Raffelt, *Phys. Rep.* **320**, 319 (1999).
- [14] M. Marinelli and G. Morpurgo, *Phys. Lett.* **137B**, 439 (1984); J. Baumann, R. Gähler, J. Kalus, and W. Mampe, *Phys. Rev. D* **37**, 3107 (1988).
- [15] S. N. Gninenko, N. V. Krasnikov, and A. Rubbia, *Phys. Rev. D* **75**, 075014 (2007).
- [16] A. Studenikin, arXiv:1302.1168.
- [17] H. B. Li *et al.*, *Phys. Rev. Lett.* **90**, 131802 (2003); H. T. Wong *et al.*, *Phys. Rev. D* **75**, 012001 (2007).
- [18] A. G. Beda, V. B. Brudanin, V. G. Egorov, D. V. Medvedev, V. S. Pogosov, M. V. Shirchenko, and A. S. Starostin, *Adv. High Energy Phys.* **2012**, 350150 (2012).
- [19] M. B. Voloshin, *Phys. Rev. Lett.* **105**, 201801 (2010); **106**, 059901(E) (2011); K. A. Kouzakov, A. I. Studenikin, and M. B. Voloshin, *Phys. Rev. D* **83**, 113001 (2011).
- [20] J.-W. Chen, C.-P. Liu, C.-F. Liu, and C.-L. Wu, *Phys. Rev. D* **88**, 033006 (2013).
- [21] W. Greiner and J. Reinhardt, *Quantum Electrodynamics* (Springer-Verlag, Berlin, 1994), Example 3.17.
- [22] B. L. Henke, E. M. Gullikson, and J. C. Davis, *At. Data Nucl. Data Tables* **54**, 181 (1993).
- [23] H. T. Wong, *J. Phys. Conf. Ser.* **39**, 266 (2006).